PHYSICAL REVIEW B **80**, 085102 (2009)

R-matrix calculation of Bloch states for scattering and transport problems

K. Varga
Department of Physics and Astronomy, Vanderbilt University, Nashville, Tennessee 37235, USA

(Received 15 April 2009; revised manuscript received 23 June 2009; published 5 August 2009)

An *R*-matrix based approach is presented to calculate complex band structure and scattering states for nanoscale transport problems. The main advantage of the approach is that the scattering states are available at all energies at once facilitating efficient transport calculations. The accuracy and the suitability of the method are demonstrated through numerical calculation of complex band structures and transmission probabilities of electron scattering in nanostructures.

DOI: 10.1103/PhysRevB.80.085102 PACS number(s): 72.10.−d, 73.40.−c, 73.63.−b, 85.65.+h

I. INTRODUCTION

Scattering states play an important role in electron transport and mobility calculations. Simulation of scanning, tunneling,[1–4] and transmission electron microscopy images[5] also requires the knowledge of scattering state solutions of the Schrodinger equation. Various methods have been developed to calculate scattering states, including Green's function-based approaches,[6–8] the transfer matrix,[9–12] and the Lippmann-Schwinger method[13–16] to mention the most popular ones. The calculation of scattering states have become a powerful tool to describe surface states, interface states, tunneling currents,[17–19] and most recently, quantum transport in nanoscale devices.[20–33] A common property of these approaches is that the scattering wave function is calculated for each desired energy, that is the calculation has to be repeated for all energy points required to describe the system. These approaches involve diagonalization or inversion of large matrices which is computationally demanding.

Another family of scattering calculations is based on the *R*-matrix theory of Wigner.[34,35] The *R*-matrix approach is mostly used in nuclear and atomic physics.[36–40] In the *R*-matrix approach one generates a complete set of basis functions (*R*-matrix functions) subject to a predefined boundary condition in a finite region and expands the wave function of the system in terms of the *R*-matrix functions. The expansion coefficients are derived from some known property of the scattering function, for example by matching to the known asymptotic form. The advantage of the *R*-matrix approach is that the scattering wave function is known for all energies at once.

In a typical scattering calculation, the Hamiltonian H is the sum of an asymptotic Hamiltonian H_0, and a scattering potential K, $H=H_0+K$. Most scattering approaches assume that the solution for the asymptotic Hamiltonian H_0 is available and proceed to find the scattering solution of H_0+K by exploiting the known asymptotic solution: the nonequilibrium Green's function calculations,[20–33] for example, use the solutions in the leads to construct the self-energy matrices of the device to calculate the charge density and the transmission probability. The transfer matrix method[9–12] propagates the asymptotic solution into the scattering region. The Lippmann-Schwinger approach[13–16] uses the asymptotic Green's function and asymptotic wave function to calculate the scattering wave function.

In scattering problems in vacuum, the asymptotic Hamiltonian is simply the kinetic energy, or the kinetic energy plus a Coulomb potential for charged particle scattering, and the asymptotic wave function is known. In scattering problems in materials (e.g., quantum transport in nanodevices or electron scattering on impurities) the asymptotic Hamiltonian H_0 is assumed to be the Hamiltonian of the crystalline material. In this case the asymptotic wave functions (Bloch functions) are not *a priori* known and have to be calculated for every energy. The efficient and accurate calculation of these asymptotic wave functions is an indispensable element of scattering calculations.

The Bloch states $\phi_k(\mathbf{r})$ have the property

$$\phi_k(\mathbf{r}) = e^{i\mathbf{k}\mathbf{r}} u_k(\mathbf{r}) \tag{1}$$

where $u_k(\mathbf{r})$ has the full crystal periodicity. In conventional band-structure calculations, the Bloch states are obtained by calculating the eigenstates of the Hamiltonian for a given crystal momentum $\mathbf{k}$. In scattering problems all $\mathbf{k}$ vectors associated with a given energy E are sought. These $\mathbf{k}$ vectors can be real or complex, the latter describing evanescent waves growing or decaying exponentially. The analytic properties of the energy spectrum of crystals as function of a complex variable have been described in Ref. 41. In the crystal, periodicity demands that the crystal momentum is real. But near a crystal surface or interface, the crystal momentum can be complex. The wave functions belonging to complex $\mathbf{k}$ vectors are particularly important in studies of tunneling currents and transport in metal insulator interfaces.

In this paper we present a powerful approach to calculate the Bloch states and complex band structure using the *R*-matrix theory. The main advantage of the approach is that the computationally demanding complex eigenvalue problem of Bloch states is transformed into an eigenvalue problem involving only auxiliary surface wave functions. The dimensionality of the surface eigenvalue problem is only a fraction of the original full eigenvalue problem and the Bloch states are available at all energies facilitating fast scattering state calculations.

Once the Bloch states are known, scattering states can be calculated using various approaches including the above mentioned transfer matrix, Green's function or Lippmann-Schwinger methods. As an illustration, we will use the *R*-matrix approach to calculate the scattering states as well.

1098-0121/2009/80(8)/085102(8)

The application of the R-matrix for calculating scattering states is well established.[36–40] The presented approach is that an essential ingredient, the asymptotic (Bloch) functions are also determined by the R-matrix approach.

The outline of the paper is as follows. First we briefly describe the R-matrix theory in Sec. II A. This is followed by the introduction of the formalism to calculate Bloch states in one- and three-dimensional systems (Secs. II B–II D). Calculation of scattering states in a nanoscale device will be briefly described in Sec. IIE, Numerical demonstration of the powerfullness of the presented approach is presented in Sec. III. The paper is concluded with a summary in Sec. IV.

II. FORMALISM

A. *R*-matrix theory

One of the most efficient approaches to solving scattering problems is the R-matrix method.[34–40] The basic idea of the R-matrix theory is to divide the system into asymptotic and interacting regions. The wave function in the asymptotic region is assumed to be known and the scattering potential is restricted to the interacting region ("R-matrix box"). By assuming fixed but arbitrary boundary conditions on the surface of the box one can solve the Schrödinger equation inside the box. The box eigenfunctions obtained in this way form a complete, discrete set of states and can be used to expand the scattering wave function at any arbitrary energy inside the box. In order to extract the scattering information (transmission probability, phase shift, etc.), the external and internal parts of the wave function are matched at the surface of the box.

In this section we briefly describe the R-matrix approach. For simplicity, we restrict the discussion to one dimension; the extension to three dimensions is straightforward. Let the interaction region be the $[a,b]$ interval and let $\Psi(x)$ denote the solution of the Schrödinger equation in the whole space

$$H\Psi(x)=E\Psi(x)H=-\frac{\hbar^2}{2m}\frac{d^2}{dx^2}+V(x)\qquad -\infty<x<\infty. \tag{2}$$

Note that H is not Hermitian on the $[a,b]$ interval because

$$\int\Psi_1(x)H\Psi_2(x)-\int\Psi_2(x)H\Psi_1(x)=-\frac{\hbar^2}{2m}[\Psi_1(x)\Psi_2'(x)-\Psi_1'(x)\Psi_2(x)]_a^b. \tag{3}$$

We also define a Green's function belonging to this Hamiltonian as

$$(E-H)G(x,x')=\delta(x-x'). \tag{4}$$

In the R-matrix theory, first an auxiliary function set $\phi_i(x)$ satisfying prescribed boundary conditions relating the wave function and its derivative at the boundary

$$\phi_i'(a)=\lambda_a\phi_i(a)\qquad \phi_i'(b)=\lambda_b\phi_i(b), \tag{5}$$

is generated inside the $[a,b]$ interval. With these boundary conditions the Schrödinger equation in $[a,b]$ becomes a discrete eigenvalue problem

$$-\frac{\hbar^2}{2m}\phi_i''(x)+V(x)\phi_i(x)=\epsilon_i\phi_i(x) \tag{6}$$

and the eigenfunctions form a complete set of states. By multiplying Eq. (2) by $\phi_i(x)$ from the left and integrating in the $[a,b]$ region

$$-\frac{\hbar^2}{2m}\int_a^b\phi_i(x)\Psi''(x)dx+\int_a^b\phi_i(x)V(x)\Psi(x)dx=E\int_a^b\phi_i(x)\Psi(x)dx. \tag{7}$$

Similarly by multiplying Eq. (6) by $\Psi(x)$ from the left and integrating in the $[a,b]$ region we get

$$-\frac{\hbar^2}{2m}\int_a^b\Psi(x)\phi_i''(x)dx+\int_a^b\Psi(x)V(x)\phi_i(x)dx=\epsilon_i\int_a^b\Psi(x)\phi_i(x)dx. \tag{8}$$

Substracting Eq. (8) from Eq. (7) one obtains

$$-\frac{\hbar^2}{2m}\int_a^b[\phi_i(x)\Psi''(x)-\Psi(x)\phi_i''(x)]=(E-\epsilon_i)\int_a^b\Psi(x)\phi_i(x)dx. \tag{9}$$

which can be further simplified by integration by parts of the left hand side, to have

$$-\frac{\hbar^2}{2m}[\phi_i(b)\Psi'(b)-\phi_i(a)\Psi'(a)-\phi_i'(b)\Psi(b)+\phi_i'(a)\Psi(a)]=(E-\epsilon_i)\int_a^b\Psi(x)\phi_i(x)dx. \tag{10}$$

By expanding $\Psi(x)$ in terms of the complete set of states $\phi_i(x)$ in the $[a,b]$ region

$$\Psi(x)=\sum_{i=1}^{\infty}c_i\phi_i(x), \tag{11}$$

the linear coefficients

$$c_i=\int_a^b\Psi(x)\phi_i(x)dx, \tag{12}$$

can be expressed using Eq. (10) and the wave function in the box is given by

$$\Psi(x)=R(b,x)\Psi'(b)-R(a,x)\Psi'(a)-R'(b,x)\Psi(b)+R'(a,x)\Psi(a) \tag{13}$$

where the "R-matrix" is defined as

$$R(x,x') = -\frac{\hbar^2}{2m}\sum_{i=1}^{\infty}\frac{\phi_i(x)\phi_i(x')}{E-\epsilon_i} \tag{14}$$

and

$$R'(x,x') = -\frac{\hbar^2}{2m}\sum_{i=1}^{\infty}\frac{\phi_i'(x)\phi_i(x')}{E-\epsilon_i}. \tag{15}$$

It is important to remember that the expansion Eq. (11) is valid on the $[a,b]$ interval but the expansion

$$\Psi'(x) = \sum_{i=1}^{\infty} c_i\phi_i'(x), \tag{16}$$

(provided that $\Sigma_{i=1}^{\infty}c_i\phi_i'(x)$ is uniformly convengent) is only valid for the (a,b) open interval (excluding the a and b end points) because in general the boundary condition is different for Ψ and ϕ_i.

Once Eq. (6) in the $[a,b]$ region is solved the R-matrix is completely known and then through Eq. (13) the wave function in the $[a,b]$ region can be calculated. Equation (13) contains the values of the wave function and the first derivative of the wave function on the boundary, but these are assumed to be available. In scattering calculations these are know from the known asymptotic wave functions. In the present work, as will be shown in the next section, these boundary values are derived from the properties of the Bloch states.

The boundary conditions defined in Eq. (5) are arbitrary and can be chosen to simplify the equations. In this work we will assume that the derivatives are zero at the boundary, so that Eq. (13) simplifies to

$$\Psi(x) = R(a,x)\Psi'(a) - R(b,x)\Psi'(b). \tag{17}$$

The simplest way to satisfy the boundary conditions is to solve Eq. (6) by expanding it using basis functions that satisfy the prescribed boundary conditions.

In a similar manner, multiplying Eq. (4) by $\psi_i(x)$ and Eq. (6) by $G(x,x')$ integrating over x in the $[a,b]$ interval and subtracting the two equations

$$G(x,x') = \frac{2m}{\hbar^2}R(x,x') + \left(R(x,b)\left.\frac{dG(x'',x')}{dx''}\right|_{x''=b} - R(x,a)\left.\frac{dG(x'',x')}{dx''}\right|_{x''=a}\right).$$

Similar equations can be derived in three dimensions, the only difference being that the values of the functions at the boundary will be replaced by the surface integral of the functions on the boundary surface and the derivatives are normal derivatives at the surface.

Alternative derivations of the R-matrix equations are also possible. To avoid the problems arising from the nonHermiticity of the kinetic energy operator in a finite region [see Eq. (3)], a boundary surface Bloch operator[42]

$$L_B = \frac{\hbar^2}{2m}\left[\delta(x-a)\left(\frac{d}{dx}-\lambda_a\right) - \delta(x-b)\left(\frac{d}{dx}-\lambda_b\right)\right] \tag{18}$$

can be introduced. Adding this operator to the Hamiltonian the resulting new Hamiltonian $\widetilde{H}=H+L_B$ is Hermitian. This Hermitian Hamiltonian can be diagonalized using an auxiliary basis function set φ_i and the eigenfunctions ϕ_i satisfy the boundary conditions prescribed in Eq. (5). One can expand the wave function $\Psi(x)$ using the eigenfunctions ϕ_i and following the steps described above one obtains

$$\Psi(x) = \sum_i \frac{\phi_i(x)\langle\phi_i|L_B|\Psi\rangle}{E-E_i} \tag{19}$$

which is equivalent to Eq. (13). The advantage of this version of the R-matrix formalism is that it can be used with auxiliary basis functions φ_i of arbitrary boundary conditions (e.g., GAUSSIANS or atomic orbitals can be used as auxiliary basis) and the Bloch operator enforces the desired boundary conditions. This Bloch operator form of the R-matrix method has been used to calculate magnetotransport properties of two-dimensional semiconductor devices in Ref. 43.

In this work we follow the first version and we expand $\phi_i(x)$ in terms of Lagrange functions.[44] The derivatives of the selected Lagrange function basis functions are zero at the boundary and the simple equation, Eq. (17), can be used to calculate the wave function. The basis functions are described briefly in the next section.

B. Basis functions

We will use Lagrange functions[44] to expand the wave function and calculate the R-matrix. The ith basis function is defined as

$$\phi_i(\mathbf{r}) = \textstyle\sum_{l=1}^{N_x}\sum_{m=1}^{N_y}\sum_{n=1}^{N_z} C_{lmn}L_{lmn}(\mathbf{r}) \tag{20}$$

where the three-dimensional L_{lmn} functions are tensorial products of one-dimensional Lagrange functions

$$L_{lmn}(\mathbf{r}) = L_l(x)L_m(y)L_n(z). \tag{21}$$

These one-dimensional Langrange functions are defined as

$$L_n(x) = \frac{1}{N} + \frac{2}{N}\sum_{k=1}^{N-1}\cos(k\pi x_n)\cos(k\pi x) \tag{22}$$

with $x_n=\frac{2n-1}{2N}$. These functions are defined on the $[0,1]$ interval and their first derivative is zero at the boundaries. Appropriate scaling must be used to map the $[a,b]$ R-matrix region and the $[0,1]$ interval. If we are interested in calculating scattering states propagating in the x direction, then only $L_l(x)$ has to satisfy the boundary conditions and the Lagrange functions in the perpendicular directions can be chosen differently. In practice, for simplicity we used the same form of basis functions in each directions.

C. Calculation of Bloch states

For a periodic potential $V(x)=V(x+L)$ (where L is the lattice vector in the x direction), the eigenfunctions are Bloch waves satisfying the fundamental property

$$\Psi_k(x+L) = \mathrm{e}^{ikL}\Psi_k(x) \tag{23}$$

$$\frac{d}{dx}\Psi_k(x+L) = \mathrm{e}^{ikL}\frac{d}{dx}\Psi_k(x). \tag{24}$$

Using these expressions and the $[a,b]=[0,L]$ interval as the R-matrix region, Eq. (17) takes the form

$$\Psi_k(x) = [R(x,b)\mathrm{e}^{ikL} - R(x,a)]\Psi_k'(a). \tag{25}$$

Taking $x=a$ and $x=b$ in this equation, using the Bloch theorem and introducing $\lambda=\mathrm{e}^{ikL}$, one obtains

$$[\lambda^2 R(b,a) - \lambda\{R(b,b)+R(a,a)\} + R(a,b)]\Psi_k'(a) = 0 \tag{26}$$

which, by defining

$$c = \frac{R(a,a)+R(b,b)}{R(a,b)} \tag{27}$$

is a second order polynomial, $\lambda^2 - c\lambda + 1 = 0$, and the roots are given by

$$\lambda = \frac{c \pm \sqrt{c^2-4}}{2}. \tag{28}$$

To test the formalism we use the analytically solvable Mathieu potential[45] and calculate the Bloch waves. The Mathieu potential is defined as

$$V(x) = V_0\left[1+\cos\left(\frac{2\pi x}{L}\right)\right] \tag{29}$$

($V_0=1.5$ Hartree and $L=5$ Bohr are used in the calculation). A simple finite difference discretization was employed to solve the Schrödinger equation [Eq. (6)]. The real and complex k vectors obtained by solving Eq. (26) are shown in Fig. 1. The calculated and analytical solutions are in perfect agreement.

D. Bloch states: Three-dimensional case

Now we are ready to present the formalism for a general three-dimensional case. We assume that the system is periodic in the y and z directions and we are looking for the Bloch states propagating in the x direction. We suppress the wave vectors k_y and k_z belonging to the y and z directions for simplicity. The calculations have to be repeated for each (k_y,k_z).

$$\Psi_k(\mathbf{r}) = \int_b R(\mathbf{r},\mathbf{r}_b')\frac{\partial\Psi_k(\mathbf{r}_b')}{\partial x'}dS' - \int_a R(\mathbf{r},\mathbf{r}_a')\frac{\partial\Psi_k(\mathbf{r}_a')}{\partial x'}dS' \tag{30}$$

where

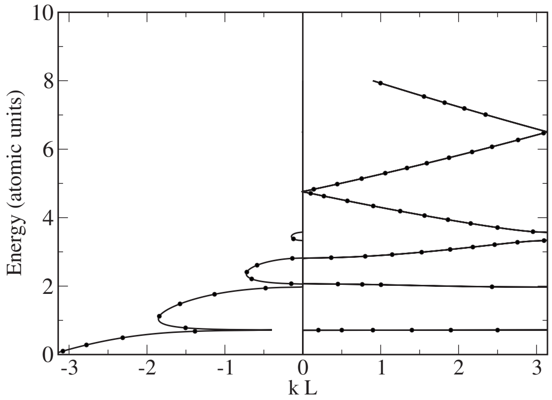

FIG. 1. Band structure calculated using the Mathieu potential. The right panel shows the real bands, while the imaginary bands are shown in the left panel. The dots show the analytically calculated dispersion values.

$$R(\mathbf{r},\mathbf{r}') = \sum_i \frac{\phi_i(\mathbf{r})\phi_i(\mathbf{r}')}{E-\epsilon_i}. \tag{31}$$

and

$$\mathbf{r}_a = (a,y,z), \quad \mathbf{r}_b = (b,y,z),$$

$$\mathbf{r}_a' = (a,y',z'), \quad \mathbf{r}_b' = (b,y',z')$$

and $dS'=dy'dz'$.

Using the Bloch theorem [as in Eq. (25)] one can rewrite Eq. (30) as

$$\Psi_k(\mathbf{r}) = \int_b [R(\mathbf{r},\mathbf{r}_b')\mathrm{e}^{ikL} - R(\mathbf{r},\mathbf{r}_a')]\frac{\partial\Psi_k(\mathbf{r}_a')}{\partial x'}dS' \tag{32}$$

and the following equation can be derived

$$\int [\lambda^2 R(\mathbf{r}_b,\mathbf{r}_a') - \lambda(R(\mathbf{r}_b,\mathbf{r}_b') + R(\mathbf{r}_a,\mathbf{r}_a')) + R(\mathbf{r}_a,\mathbf{r}_b')] \times \frac{\partial\Psi_k(\mathbf{r}_a')}{\partial x}dS' = 0. \tag{33}$$

The next step is to introduce an appropriate complete set of surface basis functions $\chi_k(y,z)$. The simplest choice is a discretization based on Dirac delta functions

$$\chi_k(y,z) = \delta(y-y_i)\delta(z-z_i) \quad (k=i,j), \tag{34}$$

or Lagrange functions

$$\chi_k(y,z) = L_i(y)L_j(z) \quad (k=i,j). \tag{35}$$

Using these surface functions Eq. (33) can be rewritten in a matrix form

$$[\lambda^2 R_{ab} - \lambda(R_{aa}+R_{bb}) + R_{ab}]X = 0 \tag{36}$$

where

$$(R_{cc'})_{ij} = \langle\chi_i|R(\mathbf{r}_c,\mathbf{r}_c')|\chi_j\rangle \quad (c=a \text{ or } b) \tag{37}$$

and

$$X_i = \left\langle \chi_i \Big| \frac{\partial \Psi_k(\mathbf{r}'_a)}{\partial x} \right\rangle \tag{38}$$

where the bracket stands for the surface integrals.

Equation (36) is a quadratic eigenvalue problem. The eigenvalues, λ_i, give the wave numbers of the Bloch states, and the eigenvectors X_i give the normal derivative of the wave function on the surface. Using these values the wave function of the system can be calculated from Eq. (32). The quadratic eigenvalue problem can be rewritten in an equivalent form as

$$\begin{pmatrix} 0 & I \\ -I & C \end{pmatrix} \begin{pmatrix} X \\ \lambda X \end{pmatrix} = \lambda \begin{pmatrix} X \\ \lambda X \end{pmatrix} \tag{39}$$

where

$$C = R_{ab}^{-1}(R_{aa} + R_{bb}). \tag{40}$$

To check the accuracy and reliability of the proposed approach we have also calculated the Bloch states using the approach described, e.g., in Refs. 32 and 46. In this approach the Bloch states are calculated by solving the equation

$$(K_0 + K_1 e^{ikL} + K_{-1} e^{-ikL})\phi_k = 0 \tag{41}$$

where

$$K_0 = H_0 - ES_0 \quad K_{-1} = H_{-1} - ES_{-1} \quad K_1 = H_1 - ES_1$$

and H_0 and S_0 is the Hamiltonian and overlap matrix of a periodic layer, while H_1 (H_{-1}) and S_1 (S_{-1}) are the same quantities calculated between two adjacent periodic layers. Note that this equation is also a quadratic eigenvalue problem, but here one has to deal with the full, three-dimensional representation and the dimensionality of these matrices are typically much bigger than those in Eq. (36).

III. SCATTERING IN A MOLECULAR JUNCTION

In this section we briefly describe how a scattering wave function of a molecular junction can be described using the present formalism. This section follows the general principles of *R*-matrix approaches[36–40] and our main purpose here is to illustrate the application of the Bloch states calculated in the previous section for scattering in a nanoscale device.

We assume that the system is divided into three regions left $L=[-\infty, a]$, center $C=[a,b]$, and right $R=[b,\infty]$. The left and right regions are assumed to be the leads consisting of periodically repeated cells. In these regions we used the approach presented in Sec. II C to calculate the Bloch functions $\Psi_k^L(\mathbf{r})$ and $\Psi_k^R(\mathbf{r})$. The wave function of the system in the leads will be linear combination of left and right moving Bloch states. Assuming an incoming wave from the left, the wave function in the lead region at energy E will take the form

$$\Psi(\mathbf{r}) = \begin{cases} \Psi_k^L(\mathbf{r}) + \sum_{k'} R_{kk'} \Psi_{k'}^L(\mathbf{r}) & \text{in } L \\ \sum_{k'} T_{kk'} \Psi_{k'}^R(\mathbf{r}) & \text{in } R. \end{cases} \tag{42}$$

In the center region we use the *R*-matrix approach to calculate the wave function

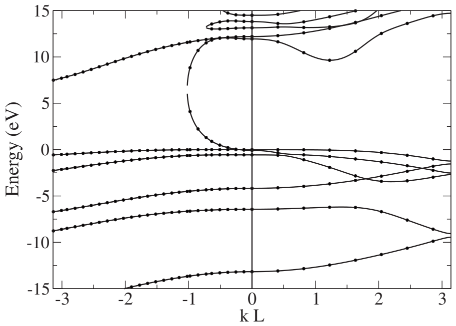

FIG. 2. Band structure of a polyethylene chain. The right panel shows the real bands, while the imaginary bands are shown in the left panel. The dots show the band structure calculated by solving Eq. (41).

$$\Psi(\mathbf{r}) = \int_b R(\mathbf{r},\mathbf{r}'_b) \frac{\partial \Psi(\mathbf{r}'_b)}{\partial x'} dS' - \int_a R(\mathbf{r},\mathbf{r}'_a) \frac{\partial \Psi(\mathbf{r}'_a)}{\partial x'} dS' \tag{43}$$

where the *R*-matrix is constructed by solving the Schrödinger equation in the central region subject to Dirichlet boundary conditions. By matching the wave functions [Eqs. (42) and (43)] on the boundary of C, a linear equation can be derived for reflection and transmission coefficients $R_{kk'}$ and $T_{kk'}$ and the wave function is determined for the whole system.

IV. NUMERICAL EXAMPLES

In the first set of examples we calculate the complex band structure of various systems. The importance of complex band structure has recently been emphasized for various nanosystems. In Ref. 47 tunneling of metal electrons through a ferromagnet-insulator-ferromagnet junction has been calculated by using the complex band structure of the insulator in the gap region. The conductance of molecular systems[17] and electron transport through double gate MOSFETs (Ref. 48) have also been studied using complex band structure calculations. Accurate tunneling currents derived from complex bands of metal-oxide-semiconductor structures have been reported in Ref. 19. The complex band structure also plays an important role in quantum transport calculations where the propagating and evanescent states of the leads have to be

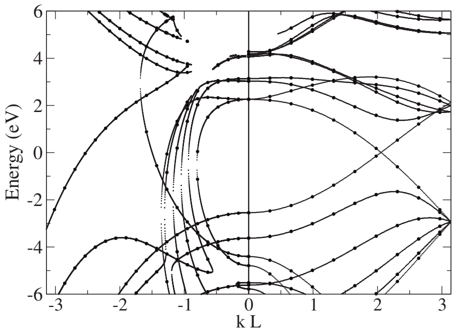

FIG. 3. Band structure of a (5,5) carbon nanotube. The right panel shows the real bands, while the imaginary bands are shown in the left panel. The dots show the band structure calculated by solving Eq. (41).

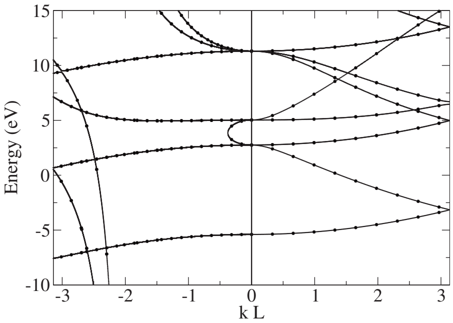

FIG. 4. Band structure of aluminum. The right panel shows the real bands, while the imaginary bands are shown in the left panel. The dots show the band structure calculated by solving Eq. (41).

known in order to calculate the transmission probability through the nanodevice.[18]

Our first example is the calculation of the complex band structure of a polyethylene chain. This system has been studied by several groups.[17,49] We have adopted the same atomic positions as given in.[49] We have used Lagrange basis functions[44] to solve the Kohn-Sham equation in the *R*-matrix box. The calculated real and imaginary bands are shown in Fig. 2. The band structure calculated by the present approach [Eq. (36)] and by solving Eq. (41) is in perfect agreement. The results also agree very well with the calculations presented in Refs. 17 and 49.

Next we present two typical examples, a (5,5) carbon nanotube and bulk Al. These systems are frequently used in quantum transport calculations either as lead or device.[25,26] Figures 3 and 4 show the calculated real and imaginary bands of a (5,5) carbon nanotube and bulk aluminum, respectively. Again, in both cases the agreement between the present approach and the conventional band structure calculation is perfect (Figs. 3 and 4). The complex band structure of the (5,5) carbon nanotube was calculated in Ref. 50. The major features of the band structure obtained in by our approach and by the tight binding method are in good agreement. Note that in the present work we solve the self-consistent Kohn-Sham equations to calculate the band structure while in Ref. 50 a parametrized tight binding Hamiltonian has been used.

In these examples, the our approach is almost three order of magnitude faster than the conventional approach (see Table I) and this presents a substantial improvement. This speed up is very advantageous in transport calculation where the calculation of the scattering wave functions in the lead has to be repeated for all energies and represent a bottleneck for the calculations.

TABLE I. Computational time (in seconds) needed to calculate the scattering wave function in one energy point for a polyethylene (PE) chain, a carbon nanotube (CN), and bulk Al.

	PE	CN	Al
Present approach solving Eq. (41)	9.8	43	91
Band-structure approach solving Eq. (39)	0.02	0.06	0.013

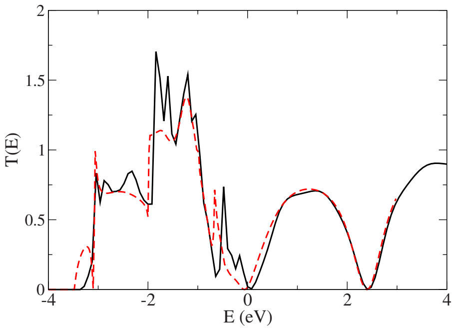

FIG. 5. (Color online) Transmission probability of a gold chain decorated by CO. The solid line is the result of the present approach while the dashed line is the benchmark result of Ref. 33.

Next we calculate the scattering wave function of a nanoscale system, a gold chain with a single CO molecule adsorbed on it. This system is studied as a benchmark system in Ref. 33. We have used the same geometry as in that paper and calculated the scattering wave function for different energies. The transmission coefficient as a function of energy is compared to the results of the benchmark study in Fig. 5. The agreement is very good, especially considering the fact that different basis functions have been used in the calculations. In Ref. 33 linear combination of atomic orbitals have been employed to represent the Hamiltonian matrix. The convergence of the scattering wave function (and, e.g., the transmission probability) on atomic centered basis function representation is slow as shown in Ref. 33. The Lagrange functions used in this work are not centered at the atoms and give a much better representation of the scattering wave function. Increasing the size of the Lagrange basis does not change the results, the transmission probability is well converged. Therefore the slight difference between the two calculations is most likely due to different representation of the scattering wave function in the two approaches.

In the last example we demonstrate the applicability of the present approach to transport problems by calculating the conductance of a carbon chain coupled to metal electrodes. The carbon chain contains seven atoms with C-C distance 1.3225 Å. The lattice constant of the Al lead is 4.05 Å. The calculated transmission spectrum is shown in Fig. 6. In this case we do not have a benchmark calculation to compare with, but the general features of the transmission spectrum are in good agreement with similar calculations.[25]

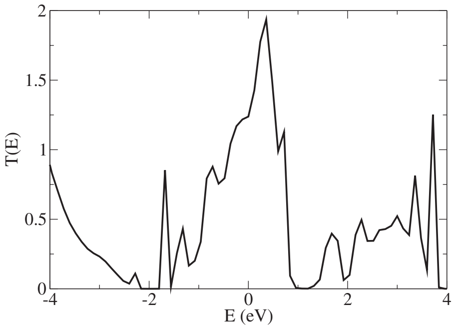

FIG. 6. Transmission spectrum of a seven atom carbon chain between Al(100) electrodes.

V. SUMMARY

We have presented an *R*-matrix approach to calculate the complex band structure and scattering states for nanoscale transport problems. The main advantage of the approach is that the scattering states at all energies are available at once facilitating efficient transport calculations.

To solve Eq. (41) on a Lagrange basis one uses $N_x \times N_y \times N_z$ basis functions, where N_x, N_y, and N_z are the number of grid points in each direction. The calculation for one energy point is then scales like $(2N_xN_yN_z)^3$. To calculate the Bloch states with the present approach using the same basis functions, one first has to solve Eq. (6) once and then solve Eq. (36) for each desired energy. The solution of Eq. (36) scales as $(2N_yN_z)^3$. Thus the present approach is roughly N_x^3 ($N_x \approx 10-20$) faster than the conventional approach. Using different bases sets would change this ratio but it is fair to say that the problem of calculating the Bloch states is reduced from three-dimensional to two-dimensional complexity.

The accuracy and the suitability of the method is illustrated through the numerical calculation of complex band structures and transmission probabilities of electron scattering. The method can be used in various calculations where the scattering wave function is required, e.g., mobility and transport calculations or simulations of electron microscopic images.

ACKNOWLEDGMENT

The work was supported by NSF grant No. ECS-0622146.

---

[1] W. A. Hofer and A. Garcia-Lekue, Phys. Rev. B **71**, 085401 (2005).
[2] K. Palotás and Werner A. Hofer, J. Phys.: Condens. Matter **17**, 2705 (2005).
[3] Kamal K. Saha, Jrgen Henk, Arthur Ernst, and Patrick Bruno, Phys. Rev. B **77**, 085427 (2008).
[4] J. Tersoff and D. R. Hamann, Phys. Rev. B **31**, 805 (1985).
[5] D. B. Williams and C. Barry Carter, *Transmission Electron Microscopy: A Textbook For Materials Science* (Springer, New York, 1996).
[6] R. E. Allen, Phys. Rev. B **20**, 1454 (1979).
[7] Y.-C. Chang and J. N. Schulman, Phys. Rev. B **25**, 3975 (1982).
[8] M. D. Stiles and D. R. Hamann, Phys. Rev. B **38**, 2021 (1988).
[9] J. N. Schulman and Y. C. Chang, Phys. Rev. B **27**, 2346 (1983).
[10] D. H. Lee and J. D. Joannopoulos, Phys. Rev. B **23**, 4988 (1981).
[11] M. Zwierzycki, P. A. Khomyakov, A. A. Starikov, K. Xia, M. Talanana, P. X. Xu, V. M. Karpan, I. Marushchenko, I. Turek, and G. E. W. Bauer, G. Brocks, and P. J. Kelly, Phys. Status Solidi B **245**, 623 (2008).
[12] K. Hirose, Nobuhiko Kobayashi, and Masaru Tsukada, Phys. Rev. B **69**, 245412 (2004).
[13] N. D. Lang, Phys. Rev. B **52**, 5335 (1995).
[14] M. Di Ventra, S. T. Pantelides, and N. D. Lang, Phys. Rev. Lett. **88**, 046801 (2002).
[15] J. Wang and H. Guo, Phys. Rev. B **79**, 045119 (2009).
[16] N. Kobayashi, M. Aono, and M. Tsukada, Phys. Rev. B **64**, 121402(R) (2001).
[17] J. K. Tomfohr and O. F. Sankey, Phys. Rev. B **65**, 245105 (2002).
[18] X.-G. Zhang, K. Varga, and Socrates T. Pantelides, Phys. Rev. B **76**, 035108 (2007).
[19] X.-G. Zhang, Zhong-Yi Lu, and Socrates T. Pantelides, Appl. Phys. Lett. **89**, 032112 (2006).
[20] S. Datta, *Electronic Transport in Mesoscopic Systems* (Cambridge University Press, Cambridge, 1997).
[21] S. V. Faleev, F. Leonard, D. A. Stewart, and M. van Schilfgaarde, Phys. Rev. B **71**, 195422 (2005).
[22] J. J. Palacios, A. J. Perez-Jimenez, E. Louis, E. SanFabian, and J. A. Verges, Phys. Rev. Lett. **90**, 106801 (2003).
[23] K. Stokbro, J. Taylor, M. Brandbyge, J.-L. Mozos, and P. Ordejon, Comput. Mater. Sci. **27**, 151 (2003).
[24] E. G. Emberly and G. Kirczenow, Phys. Rev. B **64**, 235412 (2001).
[25] J. Taylor, H. Guo, and J. Wang, Phys. Rev. B **63**, 245407 (2001).
[26] M. B. Nardelli, J.-L. Fattebert, and J. Bernholc, Phys. Rev. B **64**, 245423 (2001).
[27] Y. Xue, S. Datta, and M. A. Ratner, J. Chem. Phys. **115**, 4292 (2001).
[28] K. S. Thygesen and K. W. Jacobsen, Chem. Phys. **319**, 111 (2005).
[29] S.-H. Ke, H. U. Baranger, and W. Yang, Phys. Rev. B **70**, 085410 (2004).
[30] P. A. Derosa and J. M. Seminario, J. Phys. Chem. B **105**, 471 (2001).
[31] X. Zhang, L. Fonseca, and A. A. Demkov, Phys. Status Solidi B **233**, 70 (2002).
[32] S. Sanvito, C. J. Lambert, J. H. Jefferson, and A. M. Bratkovsky, Phys. Rev. B **59**, 11936 (1999).
[33] M. Strange, I. S. Kristensen, K. S. Thygesen, and K. W. Jacobsen, J. Chem. Phys. **128**, 114714 (2008).
[34] E. P. Wigner, Phys. Rev. **70**, 15 (1946).
[35] P. L. Kapur and R. Peierls, Proc. R. Soc. London, Ser. A **166**, 277 (1938).
[36] A. M. Lane and R. G. Thomas, Rev. Mod. Phys. **30**, 257 (1958).
[37] A. M. Lane, J. Phys. B **19**, 253 (1986).
[38] R. K. Nesbet, *Variational Methods in Electron-Atom Scattering Theory* (Plenum, New York, 1980).
[39] R. Szmytkowski, Phys. Rev. A **61**, 022725 (2000).
[40] H. Le Rouzo and G. Raseev, Phys. Rev. A **29**, 1214 (1984).
[41] W. Kohn, Phys. Rev. **115**, 809 (1959).
[42] C. Bloch, Nucl. Phys. **4**, 503 (1957).
[43] T. Jayasekera, K. Mullen, and M. A. Morrison, Phys. Rev. B **74**, 235308 (2006).
[44] K. Varga, Z. Zhang, and S. T. Pantelides, Phys. Rev. Lett. **93**, 176403 (2004).
[45] H. Statz, Z. Naturforsch. A **5A**, 534 (1950).
[46] A. R. Rocha, V. M. Garca-Surez, S. Bailey, C. Lambert, J. Fer-

rer, and S. Sanvito, Phys. Rev. B **73** 085414 (2006).

[47] Ph. Mavropoulos, N. Papanikolaou, and P. H. Dederichs, Phys. Rev. Lett. **85**, 1088 (2000).

[48] Tongsheng Xia, L. F. Register, and S. K. Banerjee, IEEE Trans. Electron Devices **50**, 1511 (2003).

[49] F. Picaud, A. Smogunov, A. D. Corso, and E. Tosatti, J. Phys.: Condens. Matter **15**, 3731 (2003).

[50] T.-S. Xia, L. F. Register, and S. K. Banerjee, Phys. Rev. B **70**, 045322 (2004).